ISSN 1070-3284, Russian Journal of Coordination Chemistry, 2016, Vol. 42, No. 1, pp. 71–80. © Pleiades Publishing, Ltd., 2016.

Syntheses, Hirshfeld Surface Analyses, and Luminescence of Four New Complexes[1]

W. P. Wu[a], *, J. Wang[a], *, L. Lu[a], B. Xie[a], Y. Wu[a], and A. Kumar[b], *

[a] *School of Chemistry and Pharmaceutical Engineering, Sichuan University of Science & Engineering, Zigong, 643000 P.R. China*

[b] *Department of Chemistry, Faculty of Science, University of Lucknow, Lucknow, 226 007 India*

**e-mail: wuweipingzg@126.com; kumar_abhinav@lkouniv.ac.in*

Received March 18, 2015

Abstract—Four Cd-based complexes with chemical formulae $[Cd(L^1)_2(2,2'\text{-Bipy})(H_2O)]$ (**I**), $[Cd(L^2)_2(2,2'\text{-Bipy}) \cdot 2H_2O]$ (**II**), $[Cd(L^1)_2(Phen)(H_2O)]$ (**III**), $\{[Cd(L^1)_2(H_2O)(4,4'\text{-Bipy})] \cdot 3H_2O\}$ (**IV**) (HL^1 = 3-(4-hydroxyphenyl)propanoic acid, HL^2 = *p*-hydroxyphenylacetic acid, Phen = phenantroline), have been synthesized and structurally characterized (CIF file CCDC nos. 1044844 (**I**), 1044844 (**II**), 1044844 (**III**), 1044847 (**IV**)). Single-crystal X-ray analyses reveal that compounds **I** and **III** have mononuclear Cd(II) units linking by three carboxylate groups, complex **II** shows dinuclear motif, whereas **IV** exhibits 1D chain constructed by bridging 4,4'-Bipy ligand. The assistant effect of chelating N-donor ligands with 2,2'-Bipy and Phen bind and bridging 4,4'-Bipy, as well as the flexibility of carboxylate, play an important to modulate on the resulting motifs. The detailed analyses of Hirshfeld surface and fingerprint plots provide insight into the nature of non-covalent interactions in the title compounds. Furthermore, the luminescent properties of the all compounds were discussed in detail.

DOI: 10.1134/S1070328416010085

INTRODUCTION

Coordination polymers (CPs) have attracted intense attention in recent years because of their intriguing structures and potential applications as functional materials [1–3]. Many efforts has been paid to the rational design of MOFs for the specific needs of applications. A conventional strategy of using long *exo*-multidentate ligands has been successful to construct frameworks with porosity [4]. Moreover, the flexible carboxylic acids are good candidates for the construction of new coordination polymers as the carboxyl groups can form C–O–M–O cyclic mode with central metal ions, thus, improving the stability of transition metal complexes [4].

On the other hands, the combination of different ligands can result in greater modulation of structural frameworks than single ligand [5–8]. Thus, mixed-ligands are undoubtedly a good choice for the construction of new polymeric structures. Furthermore, the coordination compounds with flexible ligands exhibit more complex structural feature due to the characteristics of flexible ligands [9–11]. In this report, we employed two similar and flexible carboxylates of 3-(4-hydroxyphenyl)propanoic acid (HL^1) and *p*-hydroxyphenylacetic acid (HL^2), to build complexes. We anticipated that increase architecture complexity may be introduced by using chelating or/and bridging aromatic N-donor linkers and there is an opportunity to drive the new modes of network assembly required to satisfy the unique constraints imposed by linker geometries. Furthermore, such types of the carboxylate and carboxyl groups of HL^1 and HL^2 are always actively involved in H-bonding interactions, which might turn out to be significant structure-controlling factors [12, 13]. The reactions of HL^1 and HL^2 with Cd(II) and three well-known dipyridyl linkers 2,2'-Bipy, Phen and 4,4'-Bipy under mild conditions resulted the formation of four new complexes with different motifs—$[Cd(L^1)_2(2,2'\text{-Bipy})(H_2O)]$ (**I**), $[Cd(L^2)_2(2,2'\text{-Bipy}) \cdot 2H_2O]$ (**II**), $[Cd(L^1)_2(Phen)(H_2O)]$ (**III**), $\{[Cd(L^1)_2(H_2O)(4,4'\text{-Bipy})] \cdot 3H_2O\}$ (**IV**) (Phen = phenantroline). These compounds are characterized by single crystal X-ray diffraction. Subsequently, the compounds were analyzed for their crystal packing. In order to evaluate the nature and energetic associated with intermolecular interactions in the crystal packing, the detailed analyses of Hirschfeld surface and fingerprint plots calculations were performed. The total lattice energy is partitioned into the corresponding Coulombic, polarization, dispersion and repulsion energies. Furthermore, the luminescent properties of compounds **I–IV** were discussed in detail.

[1] The article is published in the original.

Table 1. Crystal data and structure refinement information for compound **I** and **II**

Parameter	Value			
	I	**II**	**III**	**IV**
Formula weight	616.93	1213.8	640.95	670.98
Crystal system	Monoclinic	Triclinic	Monoclinic	Monoclinic
Space group	$P2_1/c$	$P\bar{1}$	$P2_1/c$	$P2_1/c$
Crystal color	Colorless	Colorless	Colorless	Colorless
a, Å	9.499(6)	11.486(4)	9.557(6)	8.7681(5)
b, Å	25.677(17)	11.567(4)	25.936(15)	15.7162(8)
c, Å	11.437(8)	11.799(4)	11.199(7)	22.5477(10)
α, deg	90	71.860(5)	90	90
β, deg	99.025(11)	70.766(5)	98.708(12)	109.664(4)
γ, deg	90	61.379(5)	90	90
V, Å^3	2755(3)	1276.8(8)	2744(3)	2925.9(3)
Z	4	1	4	4
ρ_{calcd}, g/cm^3	1.487	1.579	1.551	1.523
μ, mm^{-1}	0.840	0.908	0.847	6.484
F(000)	1256	616	1304	1376
θ Range, deg	1.97–25.19	1.86–25.20	2.00–25.20	2.15–25.60
Reflection collected	14081	6637	14159	10275
Independent reflections (R_{int})	0.0385	0.0145	0.0705	0.0807
Reflections with $I > 2\sigma(I)$	3965	4067	3148	3336
Number of parameters	351	352	369	352
R_1, wR_2 ($I > 2\sigma(I)$)*	0.0308, 0.0795	0.0280, 0.0713	0.0436, 0.0925	0.0802, 0.1756
R_1, wR_2 (all data)**	0.0422, 0.0867	0.0329, 0.0759	0.0861, 0.1152	0.1214, 0.1973

* $R = \Sigma(F_o - F_c)/\Sigma(F_o)$, ** $wR_2 = \{\Sigma[w(F_o^2 - F_c^2)^2]/\Sigma(F_o^2)^2\}^{1/2}$.

EXPERIMENTAL

Materials and method. All reagents were purchased from commercial sources and used as received. IR spectra were recorded with a Perkinlmer Spectrum One spectrometer in the region 4000–400 cm^{-1} using KBr pellets. Thermogravimetric analyses (TGA) was carried out with a Metter-Toledo TA 50 in dry dinitrogen (60 mL min^{-1}) at a heating rate of 5°C min^{-1}. X-ray powder diffraction (XRPD) data were recorded on a Rigaku RU200 diffractometer at 60 KV, 300 mA for CuK_α radiation (λ = 1.5406 Å), with a scan speed of 2°C/min and a step size of 0.013° in 2θ. Luminescence spectra for crystal solid samples were recorded at room temperature on an Edinburgh FLS920 phosphorimeter.

X-ray crystallography. Single crystal X-ray diffraction analysis of the title compounds were carried out on a Bruker SMART APEX II CCD diffractometer equipped with a graphite monochromated MoK_α radiation (λ = 0.71073 Å) by using ϕ-ω scan technique at room temperature. Data were processed using the Bruker SAINT package and the structures solution and the refinement procedure was performed using SHELX-97 [14]. The structure was solved by direct methods and refined by full-matrix least-squares fitting on F^2. The hydrogen atoms of organic ligands were placed in calculated positions and refined using a riding on attached atoms with isotropic thermal parameters 1.2 times those of their carrier atoms. The hydrogen atoms of lattice water molecule in compounds were located using the different Fourier method. Table 1 shows crystallographic data of **I**–**IV**. Selected bond distances and bond angles are listed in Table 2. Some H-bonded parameters are listed in Table 3.

Supplementary material has been deposited with the Cambridge Crystallographic Data Centre (CCDC nos. 1044844 (**I**), 1044844 (**II**), 1044844 (**III**), 1044847 (**IV**); deposit@ccdc.cam.ac.uk or http://www.ccdc.cam.ac.uk).

Hirshfeld surface analysis. Molecular Hirshfeld surfaces [15] in the crystal structure were constructed on the basis of the electron distribution calculated as the sum of spherical atom electron densities [16, 17].

Table 2. Selected bond distances (Å) and angles (deg) of structure **I**–**IV**

Bond	*d*, Å	Bond	*d*, Å
		I	
Cd(1)–O(1)	2.363(3)	Cd(1)–O(2)	2.442(3)
Cd(1)–O(3)	2.340(3)	Cd(1)–O(4)	2.538(3)
Cd(1)–O(1*w*)	2.381(3)	Cd(1)–N(1)	2.357(3)
Cd(1)–N(2)	2.409(3)		
		II	
Cd(1)–O(1)	2.339(3)	Cd(1)–O(3)	2.407(2)
Cd(1)–O(4)	2.378(2)	Cd(1)–N(1)	2.306(3)
Cd(1)–N(2)	2.328(3)	Cd(1)–O(1*A*)	2.280(2)
Cd(1)–O(2*A*)	2.554(3)		
		III	
Cd(1)–O(1)	2.510(4)	Cd(1)–O(1*w*)	2.335(4)
Cd(1)–O(2)	2.300(4)	Cd(1)–O(4)	2.303(3)
Cd(1)–O(5)	2.551(4)	Cd(1)–N(1)	2.322(4)
Cd(1)–N(2)	2.393(3)		
		IV	
Cd(1)–O(1)	2.616(7)	Cd(1)–O(2)	2.299(7)
Cd(1)–O(4)	2.425(7)	Cd(1)–O(5)	2.407(7)
Cd(1)–O(7)	2.313(6)	Cd(1)–N(1)	2.317(7)
Cd(1)–N(2*A*)	2.321(7)		
Angle	ω, deg	Angle	ω, deg
		I	
O(1)Cd(1)O(1*w*)	125.19(8)	O(1)Cd(1)O(2)	54.52(8)
O(1*w*)Cd(1)O(4)	81.42(7)	O(1*w*) Cd(1)N(1)	91.77(8)
O(1*w*)Cd(1)N(2)	148.86(8)	O(2)Cd(1)O(3)	115.61(7)
O(2)Cd(1)O(4)	160.97(7)	O(2)Cd(1)N(1)	94.40(8)
O(2)Cd(1)N(2)	123.39(8)	O(3)Cd(1)O(4)	53.29(7)
O(3)Cd(1)N(1)	147.08(8)	O(3)Cd(1)N(2)	101.61(9)
		II	
O(1)Cd(1)O(3)	85.01(8)	O(1)Cd(1)O(4)	101.13(8)
O(1)Cd(1)N(1)	88.23(10)	O(1)Cd(1)N(2)	154.19(8)
O(1)Cd(1)O(1*A*)	72.40(9)	O(1)Cd(1)O(2*A*)	119.39(8)
O(3)Cd(1)O(4)	53.62(8)	O(3)Cd(1)N(1)	104.47(9)
O(3)Cd(1)N(2)	85.70(8)	O(1*A*)Cd(1)O(3)	129.64(7)
O(2*A*)Cd(1)O(3)	148.67(8)	O(4)Cd(1)N(1)	154.48(8)
		III	
O(1)Cd(1)O(4)	121.40(12)	O(1)Cd(1)O(5)	163.53(12)
O(1)Cd(1)N(1)	88.43(13)	O(1)Cd(1)N(2)	121.39(13)
O(2)Cd(1)O(4)	89.68(13)	O(2)Cd(1)O(5)	135.43(12)
O(2)Cd(1)N(1)	120.44(14)	O(2)Cd(1)N(2)	90.45(14)
O(4)Cd(1)O(5)	53.54(12)	O(4)Cd(1)N(1)	147.60(13)
		IV	
O(1)Cd(1)O(5)	168.0(2)	O(1)Cd(1)O(7)	83.7(2)
O(1)Cd(1)N(1)	84.1(2)	O(1)Cd(1)N(2*A*)	95.8(2)
O(2)Cd(1)O(4)	85.4(2)	O(2)Cd(1)O(5)	138.3(2)
O(2)Cd(1)O(7)	134.4(2)	O(2)Cd(1)N(1)	95.7(3)
O(2)Cd(1)N(2*A*)	88.3(2)	O(4)Cd(1)O(5)	53.1(2)
O(4)Cd(1)O(7)	139.8(2)	O(4)Cd(1)N(1)	89.5(3)

Table 3. Geometric parameters of hydrogen bonds for complexes **I**–**IV***

Contact D–H···A	Distance, Å			Angle
	D–H	H···A	D···A	D–H···A, deg
		I		
O(1*w*)–H(1*wA*)···O(2)	0.83(3)	1.96(3)	2.783(4)	170(3)
O(1*w*)–H(2*wA*)···O5	0.84(2)	2.14(2)	2.948(4)	164(3)
O(5)–H(5)···O(3)	0.82	1.88	2.699(4)	176
O(6)–H(6)···O(4)	0.82	1.87	2.678(4)	166
C(8)–H(8)···O(6)	0.93	2.52	3.130(4)	123
		II		
O(1*w*)–H(1*wA*)···O(2*w*)	0.83(6)	2.14(5)	2.751(7)	131(5)
O(1*w*)–H(1*wB*)···O6	0.83(3)	1.98(3)	2.800(5)	170(3)
O(2*w*)–H(2*wA*)···O(5)	0.83(4)	1.98(5)	2.701(6)	144(4)
O(2*w*)–H(2*wB*)···O3	0.83(3)	1.96(3)	2.779(5)	168(5)
O(5)–H(5)···O(1*w*)	0.82	1.89	2.668(5)	158
O(6)–H(6)···O(4)	0.82	1.81	2.629(4)	173
		III		
O(1*w*)–H(1*wA*)···O(1)	0.83(5)	1.91(5)	2.737(6)	175(5)
O(1*w*)–H(2*wA*)···O(3)	0.83(4)	2.09(4)	2.890(6)	162(5)
O(3)–H(3)···O(4)	0.82	1.86	2.681(5)	179
O(6)–H(6)···O(5)	0.82	1.86	2.663(6)	166
C(20)–H(20)···O(1)	0.93	2.56	3.477(7)	170
		IV		
O(3)–H(3)···O(9)	0.82	1.93	2.738(9)	168
O(6)–H(6*A*)···O(1)	0.82	1.99	2.66(2)	139
O(7)–H(7*A*)···O(9)	0.85	2.00	2.820(10)	161
O(7)–H(7*C*)···O(8)	0.85	2.03	2.683(10)	134
O(8)–H(8*C*)···O(2)	0.85	1.96	2.778(10)	162
O(8)–H(8*D*)···O(6)	0.85	1.91	2.73(2)	162
O(9)–H(9*A*)···O(5)	0.85	2.15	2.762(11)	129
O(9)–H(9*C*)···O(10)	0.85	1.85	2.687(11)	170
O(10)–H(10*C*)···O(4)	0.85	1.98	2.821(10)	172

For a given crystal structure and a set of spherical atomic densities, the Hirshfeld surface is unique [16]. The normalized contact distance (d_{norm}) based on both d_e and d_i (where d_e is distance from a point on the surface to the nearest nucleus outside the surface and d_i is distance from a point on the surface to the nearest nucleus inside the surface) and the vdW radii of the atom, as given by eq. 1 enables identification of the regions of particular importance to intermolecular interactions. The combination of d_e and d_i in the form of two-dimensional (2D) fingerprint plot [18, 19] provides a summary of intermolecular contacts in the crystal [15]. The Hirshfeld surfaces mapped with d_{norm} and 2D fingerprint plots were generated using the Crystal-Explorer 2.1 [19]. Graphical plots of the molecular Hirshfeld surfaces mapped with d_{norm} used a red-white-blue colour scheme, where red highlight shorter contacts, white represents the contact around vdW separation, and blue is for longer contact. Additionally, two further coloured plots representing shape index and curvedness based on local curvatures are also presented in this paper [20].

$$d_{norm} = \frac{d_i - r_i^{vdW}}{r_i^{vdW}} + \frac{d_e - r_e^{vdW}}{r_e^{vdW}}. \quad (1)$$

Syntheses of complexes I. A mixture of $Cd(OAc)_2 \cdot 5H_2O$ (0.0412 g), HL^1 (0.0136 g), 2,2'-Bipy (0.0212 g), CH_3CH_2OH (5 mL) and deionised water (5 mL) was stirred for 30 min in air. The resulting solution was kept at room temperature for one week; the crystals

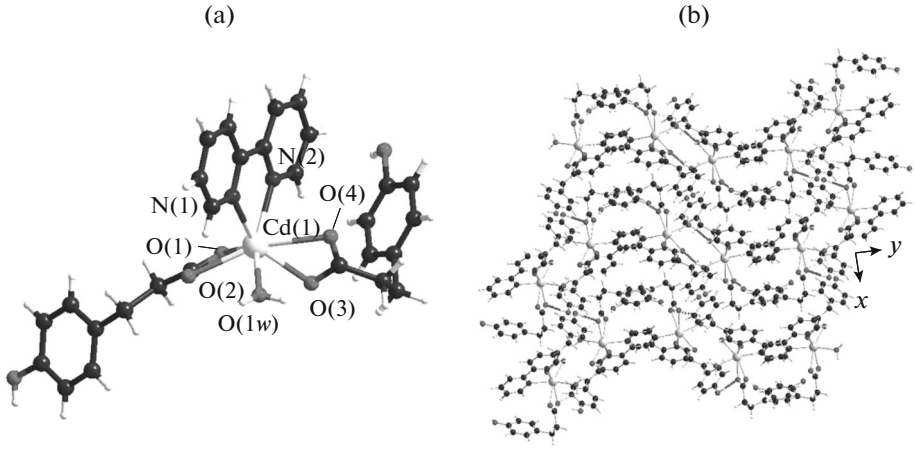

Fig. 1. The coordination geometries of the metal centers and the ligands geometries in **I** (displacement ellipsoids are drawn at the 30% probability level and H atoms are omitted for clarity) (a); view of the 2D packing framework directing by weak interactions (b).

formed were filtered off, washed with water and dried in air. The yield was 46% based on HL^1.

For $C_{28}H_{28}N_2O_7Cd$ (M = 616.92)

anal. calcd., %:	C, 54.51;	H, 4.57;	N, 4.54.
Found, %:	C, 54.31;	H, 4.32;	N, 4.42.

IR (KBr; ν, cm^{-1}): 3466 v, 3044 v, 1530 v.s, 1423 v.s, 1235 v.s, 1104 m, 990 m, 756 v.s.

Syntheses of complexes II was carried out by the same synthetic method used for **I** except that HL^1 was replaced by HL^2 (0.0156 g). The yield was 49% based on HL^2.

For $C_{52}H_{52}N_4O_{16}Cd_2$ (M = 1213.78)

anal. calcd., %:	C, 51.45;	H, 4.32;	N, 4.62.
Found, %:	C, 51.21;	H, 4.30;	N, 4.52.

IR (KBr; ν, cm^{-1}): 3477 v, 2827 m, 1577 m, 1389 v.s, 1223 m, 1001 v, 932 v, 802 m, 653 m.

Syntheses of complexes III was carried out by the same synthetic method used for **I** except that 2,2'-Bipy was replaced by Phen (0.0102 g). The yield was 51% based on HL^1.

For $C_{30}H_{28}N_2O_7Cd$ (M = 640.94)

anal. calcd., %:	C, 56.22;	H, 4.40;	N, 4.37.
Found, %:	C, 56.21;	H, 4.31;	N, 4.33.

IR (KBr; ν, cm^{-1}): 3443 v, 3038 m, 1549 v.s, 1412 v.s, 1230 m, 1104 m, 853 m, 733 m, 533 m.

Syntheses of complexes IV was carried out by the same synthetic method used for **I** except that 2,2'-Bipy was replaced by 4,4'-Bipy (0.0128 g). The yield was 41% based on HL^1.

For $C_{28}H_{34}N_2O_{10}Cd$ (M = 670.97)

anal. calcd., %:	C, 50.12;	H, 5.11;	N, 4.18.
Found, %:	C, 50.19;	H, 5.46;	N, 4.30.

IR (KBr; ν, cm^{-1}): 3523 v.s, 3181 m, 2946 m, 1611 m, 1560 s, 1435 s, 1218 m, 876 v.s, 802 s, 636 s.

RESULTS AND DISCUSSION

The results of crystallographic analysis revealed that the asymmetric unit of complex **I** contains one crystallographically unique Cd(II) atom, two L^1 ligands, one 2,2'-Bipy ligand and one coordinative water molecule. As shown in Fig. 1a, the coordinated atoms around Cd(1) is completed by five oxygen atoms (O(1), O(2), O(3) and O(4)) from two bis(monodentate) carboxylate groups, one oxygen atom from coordinative water molecule (O(1*w*)), and two N atoms (N(1) and N(2)) from two 2,2'-Bipy molecules, generating a slightly distorted pentagonal bipyramid geometry. In the CdO_5N_2 group, the Cd–O bond lengths vary from 2.339(2) to 2.538(3) Å, in which even the longest value (2.538(3) Å) is much shorter than the sum of the van der Waals radii of Cd and O atoms (2.8 Å), indicating weak Cd–O contacts [17–20]. Notably, each water ligand is H-bonded to one carboxylate of L^1 and phenolic group, and such interchain O(1*w*)···H(1*wA*)–O(2) and O(1W)···H(2*wA*)–O(5) interactions extend the discrete unit into a 1D chain. Further, such layers showing a parallel arrangement are connected by interchain O(5)···H(5)–O(3) and O(6)···H(6)–O(4) H-bonds between phenolic groups and carboxylate groups (Table 3). As shown in Fig. 1b.

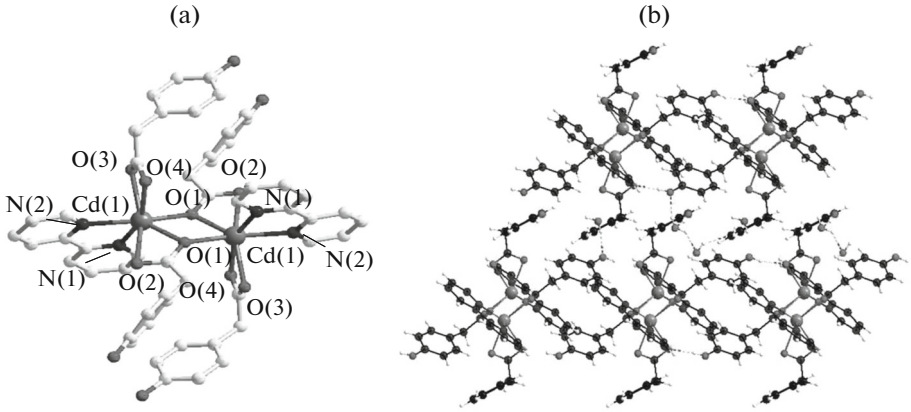

Fig. 2. The coordination geometries of the metal centers and the ligands geometries in **II** (displacement ellipsoids are drawn at the 30% probability level and H atoms are omitted for clarity) (a); view of the 2D packing framework directing by weak interactions (b).

To investigate the influence of the flexibility ligand on the complex networks, the L^1 was deliberately replaced by the little flexibility of L^2 ligand. A new compound **II** was obtained. Complex **II** displays a dinuclear unit structure. The structure of **II** contains two Cd^{2+} ions, four L^2 ligands, two chelating 2,2'-Bipy ligands, and two lattice water molecules. The two Cd(II) centers have the same geometries. Each Cd(II) atom in the dinuclear motif is coordinated by five oxygen atoms from two different carboxylic group of L^2 ligands and two N atoms from one chelating 2,2'-Bipy ligand, completing a pentagonal bipyramid geometry (Fig. 2a and Table 2). The two carboxylic groups show η^1-η^1-μ_2 and η^1-η^2-μ_2 modes.

In addition, careful analysis reveals that the hydrogen bonded interaction association of solvent water molecules, phenolic groups and carboxylate groups in **II** leads to the formation of 2D supramolecular network. The oxygen atoms (O(3) and O(4)) of carboxylate could take as acceptors to bind with O(2*w*), and O(6). The oxygen atoms (O(5) and O(6)) from hydroxyl groups acting as acceptors bind to O(2*w*) and O(1*w*), respectively. Also, the O(6) from hydroxyl group taking as donor involves in O(4) of carboxylate into a 1D chain, which are cross-lined by other H-bonded interactions between phenolic groups and free water molecules. It should be noted that there is not any packing interaction between rings from adjacent 2,2'-Bipy molecules. As shown in Fig. 2b.

To investigate the influence of the terminal ligand on the complex networks, the 2,2'-Bipy was deliberately replaced by the larger size of phen ligand. A new compound **III** was obtained. The structure of **III** is very similar with **II** (Fig. 3a), only weaker aromatic packing interactions with 4.149 Å are existed between pyridyl and benzene rings of adjacent phen ligands, as shown in Fig. 3b.

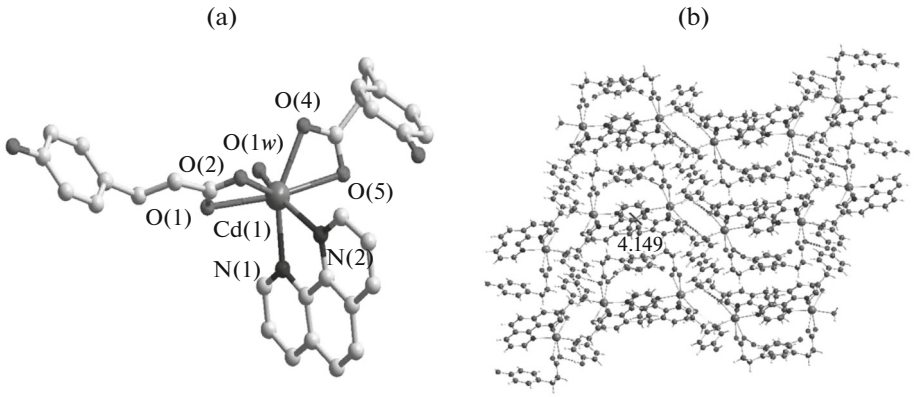

Fig. 3. The coordination geometries of the metal centers and the ligands geometries in **III** (displacement ellipsoids are drawn at the 30% probability level and H atoms are omitted for clarity) (a); view of the 2D packing framework directing by weak interactions (b).

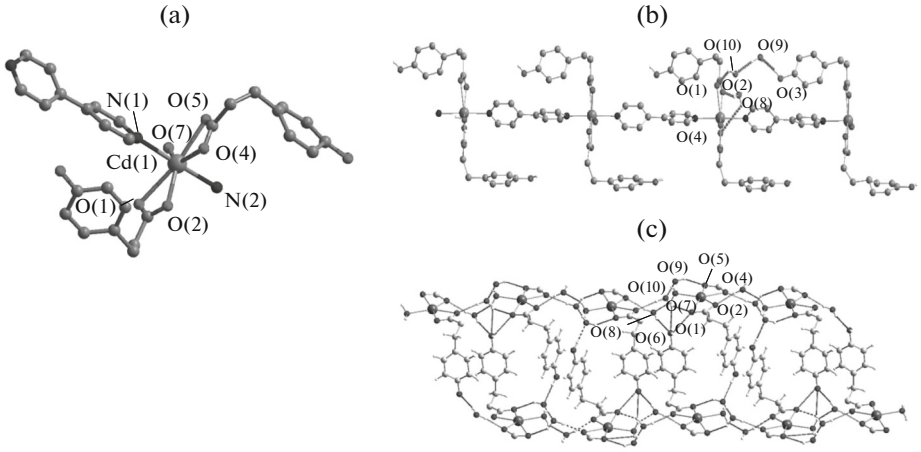

Fig. 4. The coordination geometries of the metal centers and the ligands geometries in **IV** (displacement ellipsoids are drawn at the 30% probability level and H atoms are omitted for clarity) (a); view of the 1D chain constructed by 4,4'-Bipy (b); and 1D packing chain directing by weak interactions (c).

When a bridging N-donor ligand of 4,4'-bbipy was deliberately involved in the Cd–L^1 system, a new 1D compound 4 was synthesized. The asymmetric unit of 4 consists of one Cd^{2+} ion, two L^1 anions, one neutral 4,4-Bipy, one coordinative water molecule and three free water molecules. As shown in Fig. 4a, the pentagonal-bipyramidal sphere of Cd(1) is defined by a pair of chelated carboxylate groups and one terminal coordinative water molecule in the equatorial plane, as well as two N atoms from 4,4'-Bipy at the axial sites. As a result, the 4,4'-Bipy acting as bridging linker connects the Cd centers to result in a 1D coordination motif (Fig. 4b). Whereas the L^1 ligands take as the terminal pendants to decorate the 1D array along the two sides. Notably, the coordinative water molecule O(7) is H-bonded to two free water molecules (O(8) and O(9)). Multiform H-bonds also exists between lattice water/carboxylate/phenolic, in which result in 1D chain along the *b* axis. As shown in Fig. 4c.

From a molecular level, the structural discrepancy for these complexes will be assigned to the assistant effect of N-donors and the size of carboxylate ligands [21]. For instance, the L^1 anions in **I** and **III** have the same binding mode, and the Cd centers also have the same coordinative number, whereas **I** and **III** have some different in packing modes. The resulting motifs can be viewed from the **I** and **IV** due to the assistant effect of N-donors. On the other hand, the same terminal N-donor ligand and coordinative numbers of Cd centers, the **I** and **II** have the completely coordinative architecture due to the flexibility of carboxylates L^1 and L^2.

In the FTIR spectra, all the compounds show a broad band centered around 3300 cm^{-1} attributable to the O–H stretching frequency of the water. The asymmetric stretching vibration $\nu(COO^-)$ appear around 1550 cm^{-1} for **I**–**IV**, and the symmetric stretching vibration $\nu(COO^-)$ are observed 1420 cm^{-1}. For the complexes, the difference between the asymmetric and symmetric stretches, $\Delta\nu_{as}(COO^-)-\nu_s(COO^-)$, are on the order of 150 cm^{-1} indicating that carboxyl groups are coordinated to the metal in a bidentate modes [22], consistent with the observed X-ray crystal structures of **I**–**IV**.

To study the stability of the polymers, TGA of complexes **I**–**IV** were studied. The TGA diagram of **I** shows two weight loss steps. The first weight loss began at 35°C and completed at 135°C. The observed weight loss of 3.2% is corresponding to the loss of the coordinative water molecule (calcd. 3.0%). Soon after, the deposition of all the ligands starts on. The second weight loss occurs in the range 216–750°C, which can be attributed to the elimination of L^1 and Bipy ligands. Complex **II** has also two weight loss steps. The first weight loss began at 35°C and completed at 110°C. The observed weight loss of 6.3% is corresponding to the loss of all the water molecules (calcd. 6.0%). The framework could be kept at 240°C and then start the decomposition. Complex **III** has also two weight loss steps. It can be stabilized until 115°C, and then the coordinative water molecule is removed and completed at 180°C (calcd. 2.81%, exp. 3.13%). The free water molecules are removed and completed at 98°C in **IV**, which corresponds to the loss of the coordinative water molecule (calcd. 11.2%, exp. 10.6%). The framework could be kept at 250°C and then start the decomposition.

Additionally, to confirm the phase purity and stability of compounds **I**–**IV**, all the original samples were characterized by XRPD. Although the experimental patterns have a few unindexed diffractions lines and some are slightly broadened in comparison to those simulated from single-crystal models, it can still to be considered that the bulk synthesized materi-

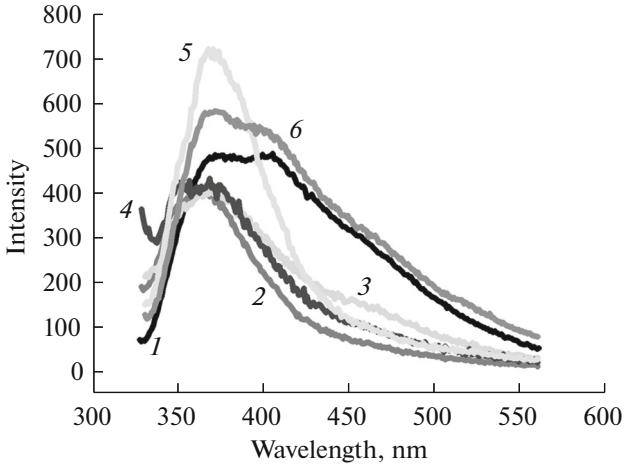

Fig. 5. View of the fluorescent emission spectra of HL^1 (*1*), HL^2 (*2*) and complexes **I** (*3*), **II** (*4*), **III** (*5*), and **IV** (*6*).

als and as-grown crystal are homogeneous for compounds **I**–**IV**.

Coordination complexes constructed from d^{10} metal centers and conjugated organic ligands are promising candidates for photoactive materials [12]. Thus, the fluorescent spectra of complexes **I**–**IV** were recorded at room temperature, which show the maximum emission bands at 362 (λ = 320 nm), 365 (λ = 320 nm), 364 (λ = 320 nm), 360 nm (λ = 320 nm), respectively. Moreover, the maximal emission of HL^1 and HL^2 ligands are observed at 361 (λ = 320 nm) and 363 nm (λ = 320 nm). Accordingly, the emission peaks of these complexes should be ascribed to interligand $\pi \rightarrow \pi^*$ and or $n \rightarrow \pi^*$ transitions. In addition, the fluorescent intensity of **III** is evidently stronger than those of HL^1 and the anslogous Cd complexes **I**, **II**

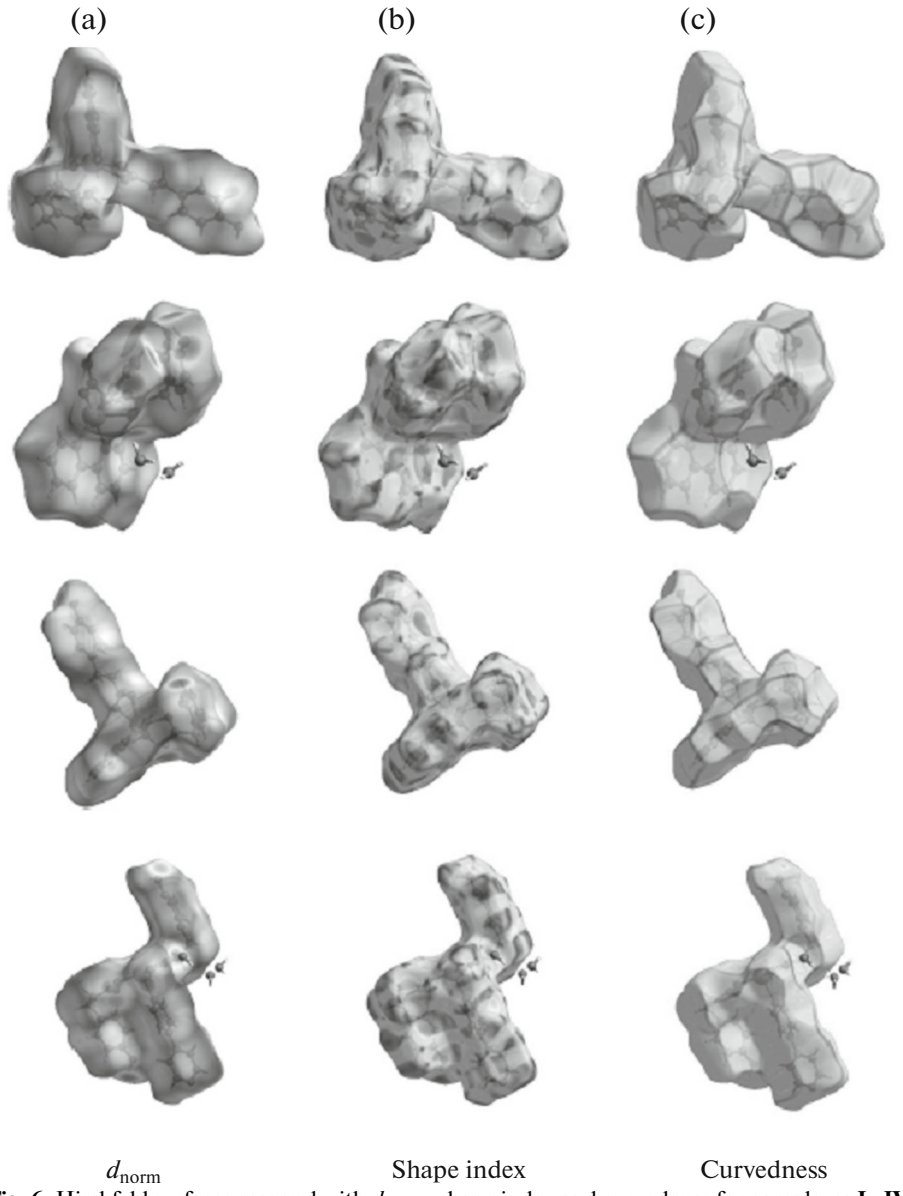

Fig. 6. Hirshfeld surfaces mapped with d_{norm}, shape index and curvedness for complexes **I**–**IV**.

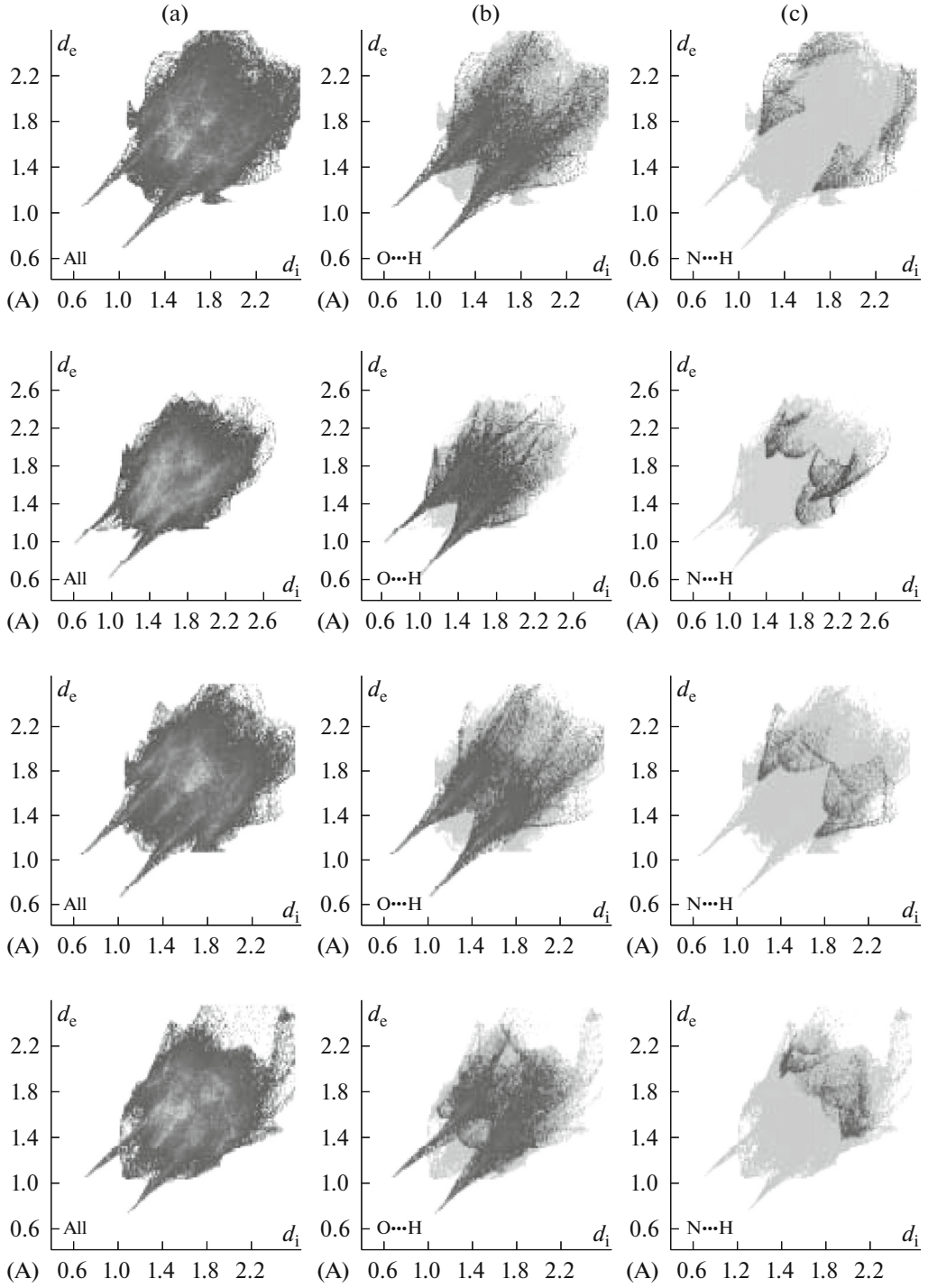

Fig. 7. Fingerprint plots Full (a), resolved into O···H (b) and N···H (c) for the complexes **I**–**IV**.

and **IV**, which may be ascribed to the conjugated effect of neutral N-donor ligands (Fig. 5).

The Hirshfeld surfaces for the complexes **I**–**IV** are illustrated in Fig. 6 showing surfaces that have been mapped over a d_{norm} range of –0.5 to 1.5 Å, shape index (–1.0 to 1.0 Å) and curvedness (–4.0 to 0.4 Å). The surfaces are shown as transparent to allow visualization of all the atoms of the molecule around which they were calculated. The weak interaction information discussed in X-ray crystallography section is summarized effectively in the spots, with the large circular depressions (deep red) visible on the d_{norm} surfaces

indicative of hydrogen bonding contacts. The dominant interactions between O–H···O for the cadmium compounds can be seen in Hirshfeld surface plots as the bright red shaded area in Fig. 6.

The fingerprint plots for **I**–**IV** are presented in Fig. 7. The O···H and N···H intermolecular interactions appear as two distinct spikes of almost equal lengths in the 2D fingerprint plots in the region 2.03 Å < (d_e + d_i) < 2.47 Å as light sky-blue pattern in full fingerprint 2D plots. Complementary regions are visible in the fingerprint plots where one molecule acts as a donor ($d_e > d_i$) and the other as an acceptor ($d_e < d_i$). The fingerprint plots can be decomposed to highlight particular atom pair close contacts. This decomposition enables separation of contributions from different interaction types, which overlap in the full fingerprint. The proportions of O···H for complexes **I**, **II**, **III** and **IV** are 23.6, 21.1, 23.5, and 21.2%, respectively of the total Hirshfeld surface while N···H interactions for complexes **I**–**IV** constitutes 2.0, 2.4, 1.9, and 2.2%, respectively of the total Hirshfeld surface [23].

ACKNOWLEDGMENTS

The authors acknowledge financial assistance from Sichuan University of Science and Engineering (nos. 2012KY12, 2014PY01, and 2015PY03), and the Education Committee of Sichuan Province (nos. 12ZA090, 13ZB0131, 14ZB0220, 15ZB0222, 15ZB0214). Abhinav is grateful to Department of Science and Technology, New Delhi for financial assistance in the form of project no. SB/FT/CS-018/2012.

REFERENCES

1. Chen, B.L., Xiang, S.C., and Qian, G.D., *Acc. Chem. Res.*, 2010, vol. 43, p. 111.
2. Carlucci, L., Ciani, G., and Proserpio, D.M., *Coord. Chem. Rev.*, 2003, vol. 246, p. 247.
3. Raymond, J. and Blankenship, R.E., *Coord. Chem. Rev.*, 2008, vol. 252, p. 377.
4. Sun, C.Y., Gao, S., and Jin, L.P., *Eur. J. Inorg. Chem.*, 2006, vol. 12, p. 2411.
5. Liu, J.Q., Wang, Y.Y., Liu, P., et al., *CrystEngComm*, 2009, vol. 11, p. 207.
6. Mondal, R., Bhunia, M.K., and Dhara, K., *CrystEngComm*, 2008, vol. 10, p. 1167.
7. Farha, O.K., Malliakas, C.D., Kanatzidis, M.G., et al., *J. Am. Chem. Soc.*, 2010, vol. 132, p. 950.
8. Du, M., Li, C.P., and Guo, J.H., *CrystEngComm*, 2009, vol. 11, p. 1536.
9. Wuest, J.D., *Chem. Commun.*, 2005, vol. 2005, p. 5830.
10. MacGillivray, L.R., *J. Org. Chem.*, 2008, vol. 73, p. 3311.
11. Kumar, A., Hüch, V., and Ram, V.J., *CrystEngComm*, 2013, vol. 15, p. 7019.
12. Badjic, J.D., Nelson, A., Cantrill, S.J., et al., *Acc. Chem. Res.*, 2005, vol. 38, p. 723.
13. Schmidbaur, H. and Schier, A., *Chem. Soc. Rev.*, 2008, vol. 37, p. 1931.
14. Sheldrick, G. M., *SHELXL-97, Program for Structure Determination and Refinement,* Göttingen: Univ. of Göttingen, 1997.
15. Spackman, M.A. and McKinnon, J.J., *CrystEngComm*, 2002, vol. 4, p. 378.
16. McKinnon, J.J., Spackman, M.A., and Mitchell, A.S., *Acta. Crystallogr. Sect. B*: *Cryst. Sci.*, 2004, vol. 60, p. 627.
17. Rohl, A.L., Moret, M., Kaminsky, W., et al., *Cryst. Growth Des.*, 2008, vol. 8, p. 4517.
18. Parkin, A., Barr, G., Dong, W., et al., *CrystEngComm*, 2007, vol. 9, p. 648.
19. Wolff, S.K., Greenwood, D.J., McKinnon, J.J., et al., *Crystal Explorer 2.0*, Perth: University of Western Australia, 2007.
20. Koenderink, J.J. and van Doorn, A.J., *Image Vision Comput.*, 1992, vol. 10, p. 557.
21. Maheshwary, S., Patel, N., Sathyamurthy, N., et al., *J. Phys. Chem. A*, 2001, vol. 105, p. 10525.
22. Nakamoto, K., *Infrared and Raman Spectra of Inorganic and Coordination Compounds*, New York: Wiley Interscience, 1997.
23. Awaga, K., Okuno, T., Yamaguchi, A., et al., *Phys. Rev. B*, 1994, vol. 49, p. 3975.